Ecological Informatics 75 (2023) 102075

Contents lists available at ScienceDirect

Ecological Informatics

journal homepage: www.elsevier.com/locate/ecolinf

Machine learning-based spatial-temporal assessment and change transition analysis of wetlands: An application of Google Earth Engine in Sylhet, Bangladesh (1985–2022)

Mirza Waleed [a], Muhammad Sajjad [a,b,*], Muhammad Shareef Shazil [c], Maham Tariq [d], Md. Tauhidul Alam [e]

[a] Department of Geography, Hong Kong Baptist University, Hong Kong Special Administrative Region
[b] Centre for Geo-computation Studies, Hong Kong Baptist University, Hong Kong Special Administrative Region
[c] Department of Space Science, University of Punjab, Lahore, Pakistan
[d] Department of Environmental Sciences, COMSATS University Islamabad, Pakistan
[e] Department of Agriculture, Noakhali Science and Technology University, Bangladesh

ARTICLE INFO

Keywords:
Machine learning
Wetlands
Change detection
Ecosystem conservation
Remote sensing applications
Google Earth Engine

ABSTRACT

Wetlands are crucial ecosystems as they enhance the quality of groundwater, protect from natural hazards, control erosion, and provide habitat to rare species of flora and fauna. Despite being valuable ecosystems, wetlands worldwide are decreasing in many regions, making mapping and monitoring of wetlands crucial. Large-scale wetlands mapping is challenging but recent advancements in machine learning, time series earth observation data, and cloud computing have opened doors to new techniques to overcome such limitations. Through evaluating the effectiveness of different classification methods, this study provides a brief analysis of wetlands dynamics in Sylhet, Bangladesh. The analysis is carried out between 1985 and 2022 using Google Earth Engine, Landsat imagery, and several spectral indices. To obtain reliable results, four classification algorithms (Random Forest, Minimum Distance, Classification and Regression Trees, and Support Vector Machine) are evaluated. As a result, Random Forest proved to be the most efficient and accurate for wetlands mapping by producing 99% accuracy across all periods. Change detection shows a rapid decrease in the wetlands in Sylhet, which could have serious consequences to the aquatic and terrestrial species, water and soil quality, and wildlife population, if not addressed. Between 1985 and 2022, nearly 45% of the wetlands have been lost in the region due to shifting land-use patterns, especially the conversion of wetlands into vegetative land (~82,000 km^2) as a result of increased agricultural practices in the region. Four critical regions (i.e., Derai, Sulla, Jamalganj, and Ajmiriganj) have undergone ~80% reduction in wetlands, requiring prompt interventions for conservation and restoration of wetlands given their diverse services.

1. Introduction

Wetlands are considered important and valuable ecosystems due to the provisioning of several services (Guo et al., 2017). Among all the natural ecosystems, wetland ecosystem services (WES) have the highest per-hectare value. Among the global ecosystems, the value of wetland ecosystem services is 47% of the total value (Xu et al., 2019). Bangladesh has many wetlands, including haors, baors, beels, freshwater lakes, marshes, rivers, streams, flooded agricultural regions, and estuarine systems with large mangrove swamps. Most of the wetlands in Bangladesh's northeast are inland (M. Islam et al., 2018), which feed many fish species, amphibians, reptiles, birds, mammals, and invertebrate species. In Bangladesh, wetland ecosystems are significant for the country's socioeconomic, industrial, cultural, and ecological well-being as nearly 50% of residents are directly dependent on wetlands (World Bank, 2016). While wetlands play a crucial role in protecting the ecology of a specific region, many factors influence the ecological balance and biodiversity of the wetland ecosystem. The major factors involved in wetland degradation are water scarcity, industrialization, urbanization, climate change, land-use changes, pollution, change in hydrological flow, and intensive agriculture practices (Chatterjee et al., 2015; Dar et al., 2020).

* Corresponding author at: Office AAB1222, Department of Geography, Hong Kong Baptist University, Kowloon Tong, Hong Kong Special Administrative Region.
E-mail address: mah.sajjad@hotmail.com (M. Sajjad).

https://doi.org/10.1016/j.ecoinf.2023.102075
Received 16 August 2022; Received in revised form 15 March 2023; Accepted 16 March 2023
Available online 24 March 2023
1574-9541/

The decline of wetlands is expected to worsen the situation in the country leading to larger flooding, intense and prolonged droughts, nutrient runoff, erosion, and a decline in the wildlife population. In the last few decades, it is estimated that due to non-conservative policies, land-use change, and climate change, Bangladesh has lost 45% of wetlands-rich areas (Islam, 2010), with varying local proportions. For instance, local studies in the Sylhet region indicate intensive environmental changes (forest loss, urbanization, agriculture), which are worsening constantly due to poor conservation policy implementation, uncontrolled overpopulation (Rashid, 2019), and extensive agriculture practices to combat food insecurity (Hoque, 2022; Sufian et al., 2017). While wetlands are crucial for Sylhet's ecosystem stability, they are not well documented and managed. To avoid the damage from becoming irreversible, it is crucial to map the state of wetlands and prepare a wetlands inventory, which can ensure its long-term monitoring and conservation (Guo et al., 2017). Besides this, multi-temporal wetlands change data (if available) allow transparency to countercheck government actions and policies for wetlands conservation assuring sustainability (Mahdianpari et al., 2020a, 2020b).

In the past, policymakers relied solely on field surveys for the monitoring of wetlands. While this process is acceptable, it has many shortcomings including a high cost for labor work, time constraints, and finding experts in such fields to carry out surveys. Due to this, developing regions, such as Sylhet in Bangladesh, lack proper survey facilities (Hoque, 2022). Conversely, remote sensing (RS) provides means to monitor long-term wetland situations using satellite-based multi-temporal data (Mallick et al., 2021). RS is a cost-effective technique compared to conventional field surveys and provides multi-spatial and multi-temporal information (Amani et al., 2019b). Furthermore, frequent and freely accessible satellite data allow researchers to study multi-temporal land use and land cover (LULC) trends with reasonably good accuracies (Waleed and Sajjad, 2022). Though there are numerous freely available satellite datasets, each has its advantages and drawbacks. For multi-temporal change studies, optical satellite data such as the Landsat archives are preferred because of their availability since the 1970s and high revisit time (Kaplan et al., 2019). While remote sensing techniques are favorable for wetlands mapping, many associated challenges need to be addressed first. These include higher computation power required for large-area classification, poor weather conditions during image acquisition, and classification errors due to intermixing of similar land-use classes having similar spectral signatures (Guo et al., 2017). While such issues are unavoidable, recent advancements in satellite sensors and data processing techniques permit overcoming such hurdles (Bhowmik, 2020; Masoud Mahdianpari et al., 2020a; Ståhl and Weimann, 2022).

Google Earth Engine (GEE) is a cloud platform well known for its cloud-based large-scale computation capabilities. Among many other applications, it facilitates land-cover assessment on large scales (Prasai et al., 2021). Provided freely for educational purposes by Google, this platform allows analyzing geospatial data using a browser-based interface and JavaScript programming language (Tamiminia et al., 2020). As GEE hosts petabytes of satellite data from multiple sources, it becomes handy to run spatial modelling over a large area and get instant output. Besides this, GEE also supports the implementation of machine learning (ML)-based models known as classifiers. These classifiers allow supervised classification to be more robust (Mahdianpari et al., 2020a, 2020b). Despite many advancements in remote sensing techniques, the classification of wetlands is still a challenging task to perform. The main reason for this difficulty is the ecological similarities between different land use types (Anand and Oinam, 2020). While there are some ML-based algorithms with proven good accuracies in land-use classification, they need to be compared based on the geographical region to assess their true classification potential (Amani et al., 2019a).

However, given the number of classifiers available, the choice of an optimal approach becomes challenging. Random Forest (RF) algorithm is designed on the decision trees principle with each node casting an individual vote and classification is decided by a majority of votes' decision (Waleed and Sajjad, 2022). It is a well-developed classifier, which is robust and is not affected by the noise in training data (Pelletier et al., 2016). Minimum Distance (MD) classification algorithm, as the name indicates, is established on the principle of unknown image data categorization from the least distance of multi-feature space (Talukdar et al., 2020). As the MD classifier works on Euclidean distance, it is comparatively faster in the classification of the training dataset in comparison with other well-known classifiers. Classification and Regression Tree (CART) method is also established on the decision tree principle except in its case, every fork is a split in a predictor variable and each last node contains a prediction for the outcome variable (Mahdianpari et al., 2020a, 2020b). CART requires minimum data modification and filtering, and with minimum supervision, it can find interactions and data discontinuity (Sang et al., 2019). The Support Vector Machine (SVM) algorithm is designed on the group classification principle where it categorizes data belonging to each category with minimum available training samples. It is fast and well suited to relatively low sample sizes with a high degree of dimensional spaces (Mahdavi et al., 2018).

Previous literature (e.g., Hassan, 2017; Md. N. Islam et al., 2018; and Salauddin and Islam, 2011) indicates wetlands degradation in Sylhet but to our knowledge, no study has provided a detailed framework-based assessment of wetlands mapping and change detection—hindering conservation and effective monitoring. Thus, this study utilizes state-of-the-art geospatial modelling approaches to (a) map multi-temporal wetlands (b) pixel-based change detection analysis to highlight wetlands gain or loss trends, (c) change transition analysis to identify contributing factors for wetlands decline if any, and (d) aggregate wetlands gain or loss as percent change for each Upazila (sub-district) in Sylhet to inform local authorities. The outcomes from this study will establish the first-of-its-kind wetlands inventory for this region. This would allow concerned departments to monitor previous and current government policies and initiatives towards wetlands conservation in the region and to initiate wetlands restoration programs in those sub-districts where wetlands showed a major decline over the last decades.

2. Methodology

2.1. Study area

The study area encompasses the entire Sylhet division located in the northeastern part of Bangladesh. Geographically, the region is surrounded by hillocks and lies between latitude 23°59′N to 25°12′N and longitude 90°27′E to 92°30 E (Fig. 1). The region's climate is a subtropical monsoon. The rainy season, which lasts from April to October, is hot and humid, with frequent heavy showers and thunderstorms. On the other hand, the short dry season, which lasts from November to February, is warm and relatively clear. Compared to the country's annual average rainfall, the northeastern region has the highest rainfall and the lowest temperature. The region's average annual temperature and rainfall are 23.6 °C and 5048 mm, respectively (Haque et al., 2017). Wetlands are the main ecosystem of the entire division. It is estimated that the core haor area (also known as the Sylhet haor basin) is spread over an area between 4450 km^2 and 25,000 km^2 (Haque et al., 2017; Iqbal et al., 2015). Sylhet is well known for one of the largest wetland areas in Asia, Hakaluki Haor. With an area of 18,386 ha, it is home to some rare fish species that have been listed as vulnerable and endangered (Iqbal et al., 2015). This system also protects lower floodplains from flash floods. Additionally, wetlands beautify their surrounding landscape during the monsoon and hot seasons (Chowdhury et al., 2022; Iqbal et al., 2015).

2.2. General workflow

This study was carried out through various steps including data acquisition, pre-processing, feature extraction, classification, accuracy

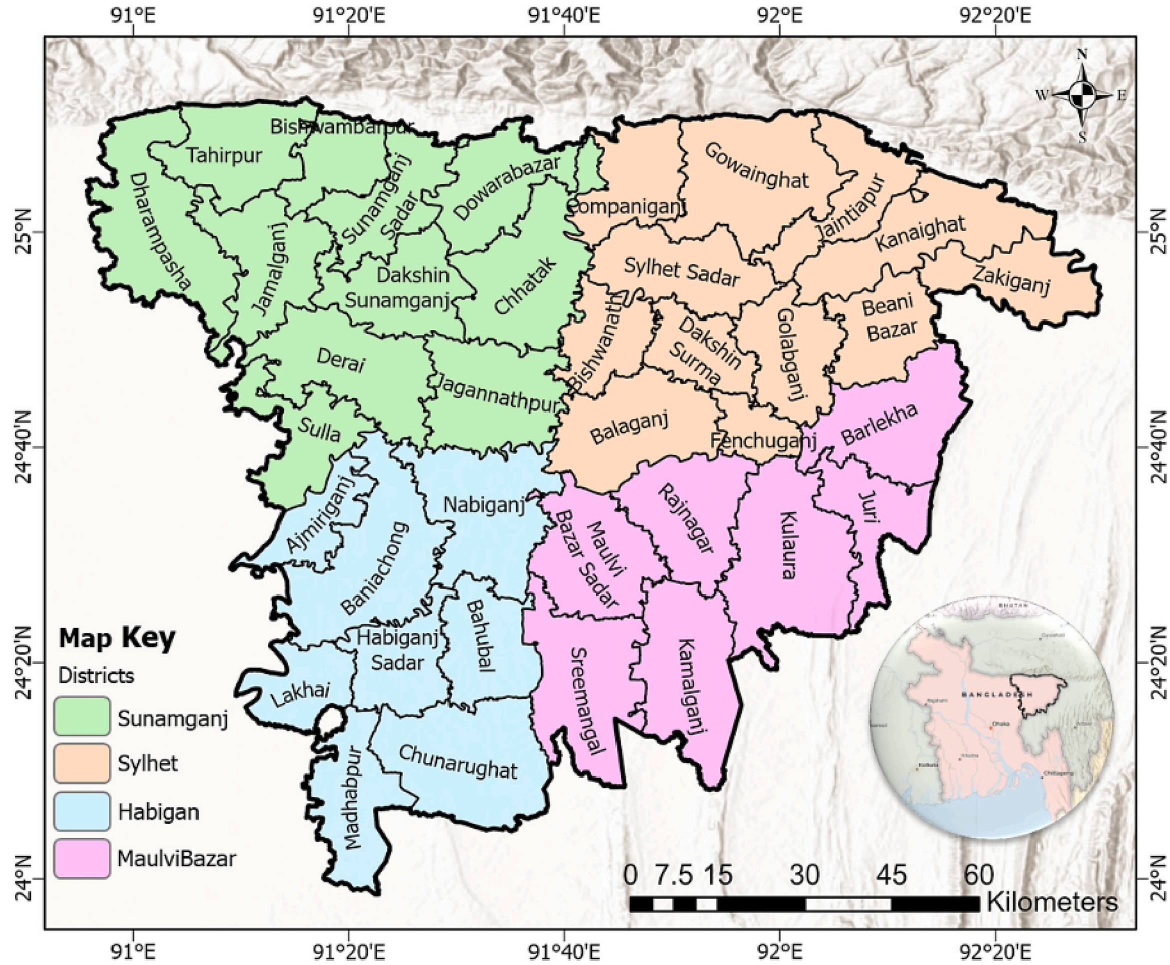

Fig. 1. Study area map of Sylhet Division

assessment, and change detection. Overall, the methodology consists of two sections. The first section comprises the use of GEE for satellite data acquisition, pre-processing, feature extraction, and collecting training and validation data. The second section consists of using GEE for ML-based wetland classification, accuracy assessment, and change detection. The overall methodology adopted in this study is presented in Fig. 2.

For spatial-temporal assessment of wetland areas, we choose Landsat satellite data available inside the GEE data catalogue (https://developers.google.com/earth-engine/datasets). While other datasets are available, they either lack good resolution or sufficient time coverage. Since Landsat satellite data are available after the 1970s, we used Landstat-5 Thematic Mapper (TM) tier-1 Surface Reflectance (SR) and the Landsat-8 Operational Land Imager (OLI). Using these two satellite instruments, five image composites were prepared. The first three (1985–87, 1995–97, 2005–07) were prepared using Landsat 5 TM data, whereas the last two (2015–17, and 2020–22) were prepared using Landsat-8 OLI data. Since wetland changes occur seasonally, we filtered satellite images only in the first three months (January, February, and March). As Sylhet lies in a tropical region making it prone to cloud coverage, we filtered all images below 10% cloud coverage to ensure data quality. Overall, 235 images were acquired for the analysis presented in this study. The details of composites and filtered images are given in Supplementary Table S1. Cloud masking was performed on the filtered images using the quality assessment band of Landsat (Waleed and Sajjad, 2022). This step ensures that only pixels without cloud presence are further taken for processing, which greatly improves the input data quality. After this, all cloud-masked images were aggregated into one image using the median pixel of each cell of the figures composite. For this operation, the *".median()"* function of GEE was applied to all the resultant cloud-masked images.

2.3. Preprocessing

Land-use classification results can be improved using Spectral Indices (SIs) (Hislop et al., 2018). SIs are preferred mostly due to their ability to differentiate certain earth's features (i.e., vegetation cover, barren land, and water cover). Besides, they are well-recognized for reducing the influence of atmospheric and topographic noise (Waleed and Sajjad, 2022). Therefore, based on the literature, we utilized the top five wetlands SIs including the Normalized Difference Vegetation Index (NDVI), Normalized Difference Built-up Index (NDBI), Modified Normalized Difference Water Index (MNDWI), Enhanced Vegetation Index (EVI), and Land Surface Water Index (LSWI). In GEE, these SI's were prepared and added to each of the five composite images using the *"addBands()"* function of GEE. As these are very common SIs in the field, further detail of each SI is given in Table S2. Before feeding these SI's to our classifier, we performed collinearity and variable importance analyses. The collinearity analysis cross-checks the correlation of the input variables supplied to the ML model and ensures that the model remains unbiased in making end decisions (Waleed et al., 2023). The lowest collinearity was found among MNDWI, NDVI, LSWI, NDBI, and EVI, and therefore were selected for further assessment.

The variable importance analysis sorts each feature based on its predictive power (Mahdianpari et al., 2020a, 2020b). The resulting variable importance statistics show the features (including SI's and

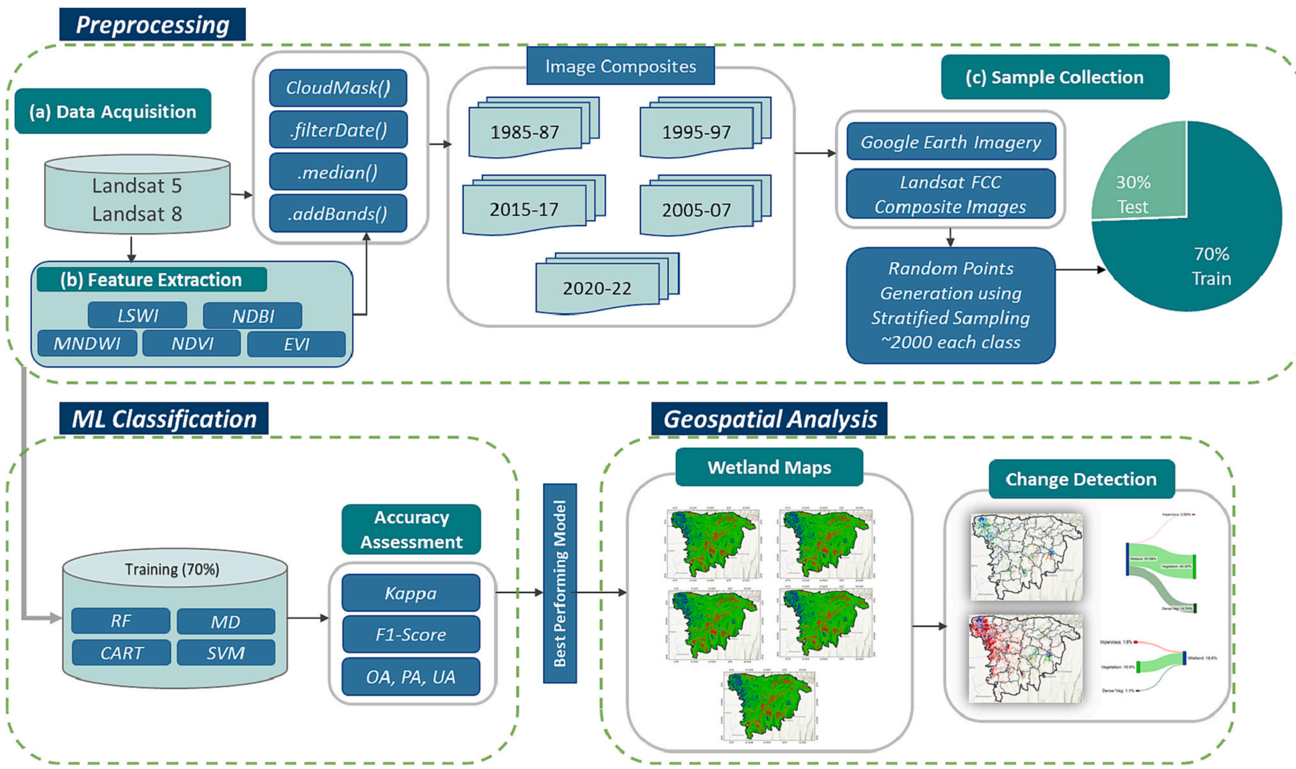

Fig. 2. Methodology flowchart representing the overall workflow followed in this research (i.e., preprocessing, ML-based classification, and geospatial analysis).

image bands) which played a crucial role in classification and vice versa. For this study, we feed 10 features to our ML classifiers including Landsat bands (Blue, Green, Red, Near-Infrared (NIR), and Shortwave-Infrared (SWIR)) along with SIs (MNDWI, NDVI, LSWI, NDBI, and EVI). Due to the unavailability of a wetland inventory database and field survey data, this study focused primarily on satellite-derived samples. Four general land-use classes consisting of impervious, vegetation, wetland, and dense vegetation are selected, details of which are given in Table 1. After this, using multiple auxiliary data sources (Google Earth Imagery and Landsat False Color Composite (FCC) Images) and respective Landsat composite images (Fig. 2), we collected ~2000 samples for each class in the form of point or polygon inside GEE. The methods used for providing the training and testing sampling data must be carefully considered as ML-based classifiers use pre-labelled samples to train models and are sensitive to uneven training datasets (Dronova, 2015).

Conventionally, various sampling techniques are used to acquire samples that were further utilized for training/validation purposes. Some of the most commonly used sampling approaches include random, systematic, and stratified sampling (Talukdar et al., 2020). The main problem with using random sampling is that it selects pixels randomly creating a high probability of missing out particular locations or group of samples. This may generate a bias in the training dataset (Hu et al., 2021). On the contrary, systematic sampling requires a close approximation of data and is less random (Waleed et al., 2022). Thus, stratified sampling was used in this study. This approach divides data into subgroups where each subgroup is randomly sampled. Hence, this approach helps to obtain accurate estimation for all the land-use classes. After collecting samples for each year and each class, 70% of the samples were used to train an ML-based classifier and 30% of the samples were used for validation—accuracy assessment.

Table 1
The description of land cover classes in Sylhet Division, Bangladesh.

Land use class	Description
Impervious	Residential areas, industrial areas, transportation, communications, mixed urban, and other urban areas, bare soil, sandy areas, strip mines, bare rock
Wetland	Wetlands, inland water bodies, rivers, reservoirs, lakes, low-lying areas
Vegetation	Cultivated land, fallow land, and terraces
Dense vegetation	Deciduous forest land, evergreen forest land, mixed forest land, grassland, orchard, and urban green areas

2.4. Machine learning-based classification

There are many methods for the classification of wetlands, but recent studies suggest RF, MD, CART, and SVM classifiers perform better than others (Dronova, 2015; Guo et al., 2017; Mahdavi et al., 2018). Hence in this study, we initially utilized these four algorithms and evaluate their wetland classification potential in the study area. Then, the best-performing algorithm (based on accuracy) was used for further multi-temporal wetland classification and change detection. Among these algorithms, default tuning parameters provided by GEE were assigned to MD, CART, and SVM for classification. For the RF algorithm, the number of trees value was a required input, which was set to 115 as determined in the literature (Shafi et al., 2023).

2.5. Post-classification procedures

Post-classification includes accuracy assessment, area statistics, wetlands change analysis, and administrative unit-level assessment of wetlands. To assess the performance of the aforementioned ML classifiers and the quality of results, it is necessary to perform an accuracy assessment (Rwanga and Ndambuki, 2017). In this study, the Kappa coefficient (K), F1-Score (F1S), Overall Accuracy (OA), Producer Accuracy (PA), and User Accuracy (UA) were used to evaluate the performance of a classifier. The accuracy metrics were calculated in GEE and the outcomes were based on the confusion matrix. The confusion matrix is a table that defines the performance of classification by analyzing the values of true positive, true negative, false positive, and false negative classified pixels (Waleed and Sajjad, 2022). Furthermore, we produced heatmaps to graphically represent the confusion matrix using the Seaborn library of Python (see details at https://seaborn.pydata.org/). The equations used to derive different accuracy metrics are provided in Table 2. For area estimation of each class, we utilized GEE's built-in command "*ee.Image.pixelArea()*".

To analyze multi-year wetlands change, the change detection technique was employed. Change detection involves pixel-by-pixel comparison of multi-year classified thematic maps (Waleed and Sajjad, 2022) and is an important part of satellite image classification as it provides environmental monitoring applications, such as change transition and natural resource depletion in space and time (Adam et al., 2010).First, wetland change analysis (statistics based) was performed by subtracting pre-area (the initial year for each LULC class) from post-area (the final year for each LULC class). For raster-based change analysis, ArcGIS Pro V3.0 was used (available at https://pro.arcgis.com/). Specifically, the "*Change Detection Wizard*" (an ArcGIS Pro tool) was used to analyze the changing patterns in wetlands over multiple years. Similarly, for change transition analysis (i.e., which wetland area converts into which land use class), the same tool was used. Lastly, for the assessment at administrative unit levels, the change detection was performed in each Upazila using the ArcGIS Pro tool called "*Zonal statistics as table*". This tool provides area change statistics, which were then imported to the Upazila vector file using the "*Join*" tool in ArcGIS Pro.

3. Results

3.1. Machine learning-based classification

To assess the effectiveness of wetland mapping, classification is conducted using different methods including RF, CART, MD, and SVM. The results from these methods are compared for the 2020–22 composite as illustrated in Fig. 3a. The comparison shows that only MD shows an overestimation of the impervious class, whereas RF, CART, and SVM show a similar distribution of land-use classes. Supplementary Table S3 represents the accuracy of each classification method (in all classes) for all five composites (1985–2022). Among all the methods, RF showed the highest accuracy to classify each class (OA = 0.99 and K = 0.99). On the other hand, MD showed the lowest accuracy of 0.72 and 0.76 for K and OA, respectively. The accuracy results of CART and SVM are in between with OA and K of 0.78 and 0.81, respectively.

Fig. 3b shows the heat maps representing the actual and predicted pixels of classified maps for each composite between 1985 and 2022. Fig. 3c shows bar plots of K, F1s, UA, PA, and OA of RF classification (best performing model), with an average accuracy of 98%. The heat maps represent accuracy maintained by RF while identifying different classes efficiently with only a 2% margin of error. The variable importance ranking highlights the most useful variables (SIs and Landsat bands), which contributed to the increase in the efficiency and accuracy of the classification results (Fig. 4). Fig. 4a shows the overall ranking, in which NDVI, MNDWI, and EVI reflect the highest ranking. NDBI and

Table 2
Accuracy assessment metrics used in this study.

Name	Abbreviation	Equation	References
Kappa Coefficient	K	$K = \frac{p_o - p_e}{1 - p_e}$	(Cohen, 1960)
F1-Score	F1S	$2 \times \frac{PA \times UA}{PA + UA}$	(Sasaki, 2007)
Overall Accuracy	OA	$\frac{TP + TN}{TP + TN + FP + FN}$	(Congalton, 1991)
Producer Accuracy	PA	$\frac{TP}{TP + FN}$	
User Accuracy	UA	$\frac{TP}{TP + FP}$	

where p_o is a relative observed agreement, p_e is the probability of chance, TP is true-positive, TN is true-negative FP is false-positive, and FN is false-negative.

Green band, on the other hand, show the lowest one. The heatmap shows the multi-year efficiency of variables, making it prominent that the highly efficient variables are NDVI, MNDWI, and EVI for each period (Fig. 4b).

3.2. Wetland distribution in the study area

The classified maps of the study area generated by RF for five composites are shown in Fig. 5. The land use map for 1985–87 shows that the north-western part is dominated by wetlands with some fragments of impervious surface and vegetation with the greatest land coverage in the region, see Fig. 5(a). Based on the classified maps as shown in Figs. 5b-e, the land coverage in four decades has significantly changed due to transitions among different classes. The loss of wetlands is more significant from 1995 to 97 to 2005–07 (Figs. 5a and b) though there is a slight increase in wetlands from 2005 to 07 to 2015–17 (Figs. 5c and d). The increase in impervious coverage in the northeastern part and the shift of wetlands from the western to the eastern part of the region from 2020 to 22 are also observed, see Fig. 5e. Notably, the loss of wetlands is significant across the study period.

3.3. Wetlands change analysis

3.3.1. Inter-decadal change detection

Fig. 6 highlights the change detection in wetlands per decade. For instance, Figs. 6a and b depict that wetlands experienced a massive loss (~30%, Supplementary Fig. S1) in area coverage from 1985 to 1995 and a mediocre loss from 1995 to 2005, respectively (represented in red shades). In addition to the loss of coverage in the first two decades, the wetland gain can also be seen during 2005–15 (Fig. 6c), where the wetlands have been recovering (~11%, Supplementary Fig. S1b), especially in northwestern part. Fig. 6d illustrates the increasing trend of wetlands in the eastern part of the region (green shades). Overall, the geographical distribution of gain and loss of wetland regions for the entire period (1985–2022) is presented in Fig. 6e with higher concentrations of wetland loss in northwestern areas (overall ~45% loss as depicted in Supplementary Fig. S1b).

3.3.2. Transitions in wetlands during 1985–2022

The conversion of wetlands to non-wetland classes and vice versa is evident during 1985–2022 (Fig. 7). Fig. 7a illustrates vegetation as a significant contributor to the wetland's loss in the first decade (1985–95). Fig. 7b shows the loss of wetlands as a result of significant conversion to vegetation and minor conversion to impervious and dense vegetation. Fig. 7c represents the conversion of vegetation and dense vegetation to wetlands that led to the increase in land coverage of wetlands. Fig. 7d also represents the transitional changes in the most recent decade (i.e., 2015–22) with a net gain of wetlands because of the rare conversion of non-wetland classes to wetlands. Finally, Fig. 7e explains the overall transitional changes over the four decades with a significant loss of area coverage in the western part and a slight gain in area coverage in the eastern part of the study area.

The transitions are further quantified to evaluate the state of land cover change during 1985–2022 (Fig. 7). Sankey diagram (Fig. 7f) illustrates that over the past four decades, wetlands were reduced. Of these, 49% are converted to vegetation, 15% to dense vegetation, and only 1% to impervious. Hence, it is obvious that the transition to vegetation land cover (having a major proportion of agricultural land, Table 1) is the most important factor responsible for the loss of wetlands in the region followed by dense vegetation. Fig. 7f further explains the conversion of other classes to wetlands (wetland gain). Based on the results, an 18% increase in the overall wetland coverage has been recorded due to the conversion of 15.9%, 1.8%, and 1.1% vegetation, impervious, and dense vegetation, respectively. Fig. 7g reveals the decadal variations in the area for each class from 1985 to 2022. Area-wise, the highest area change flow was observed from the wetland to

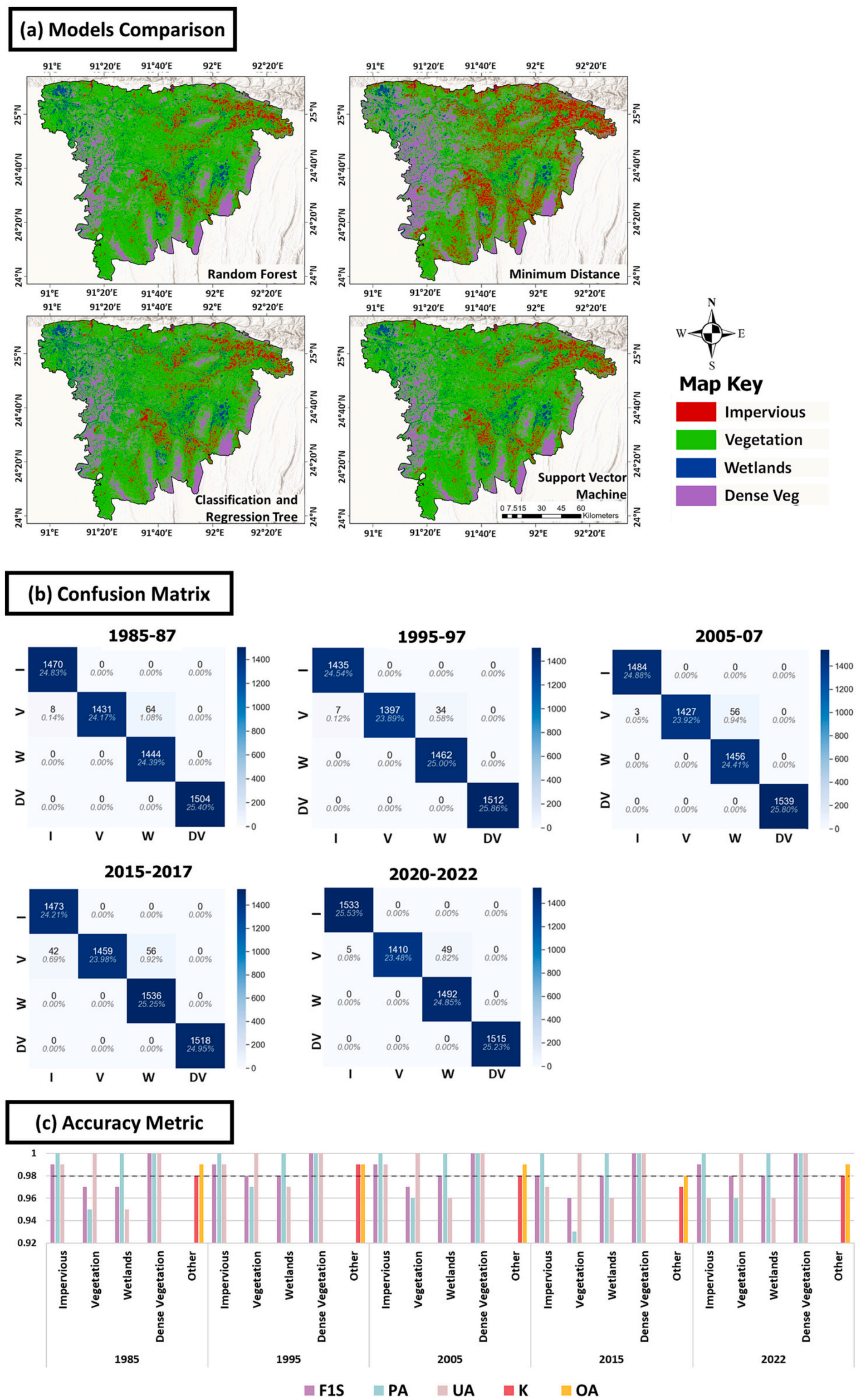

Fig. 3. The Figure is divided into three sections (a-c). The first section (a) shows the comparison of different models for wetlands classification using the 2020–22 composite image. The second section (b) shows heatmaps based on the confusion matrix of the best-performing Random Forest (RF) model for each composite image (1985–2022). The confusion matrix-based heatmaps represent the relationship between actual and predicted pixels of wetlands classification maps for 1985–2022 composites. These heatmaps are produced using the Seaborn library of python (https://seaborn.pydata.org/) and axis names include Impervious (I), Vegetation (V), Wetlands (W), and Dense Vegetation (DV). The last section (c) shows the detailed accuracy assessment of wetlands maps using accuracy metrics i.e., the Kappa statistics (K), Overall Accuracy (OA), F1-Score (F1S), Producer Accuracy (PA), and User Accuracy (UA). The dotted horizontal line in (c) is for reference accuracy values >0.98.

vegetation class. Wetlands area converted into vegetation is nearly 61,000 km^2 (1985–1995), 51,000 km^2 (1995–2005), 31,000 km^2 (2005–2015), and 39,000 km^2 (2015–2022), see Fig. 7g. However, for the overall (1985–2022) change transition, nearly 82,000 km^2 of wetland area is converted into vegetative land, showing that agriculture-based anthropogenic activities resulted in wetland loss.

To represent the loss and gain of wetlands in sub-districts (Upazilas) of the study area, a thematic map is produced (Fig. 8). In general, the overall western side of the Sylhet division shows wetland loss trends, whereas the eastern side shows wetland gain trends. Precisely, ~80% of wetlands have been lost in the western Upazilas. In particular, Derai, Sulla, Jamalganj, and Ajmiriganj faced intensive losses in wetland area coverage. However, most of the eastern Upazilas have experienced an increase in the area coverage between 70% to 200%, while a few Upazilas have maintained the wetlands and some with a slight increase in area. Gowainghat, Juri, and Kulaura are the most prominent Upazilas

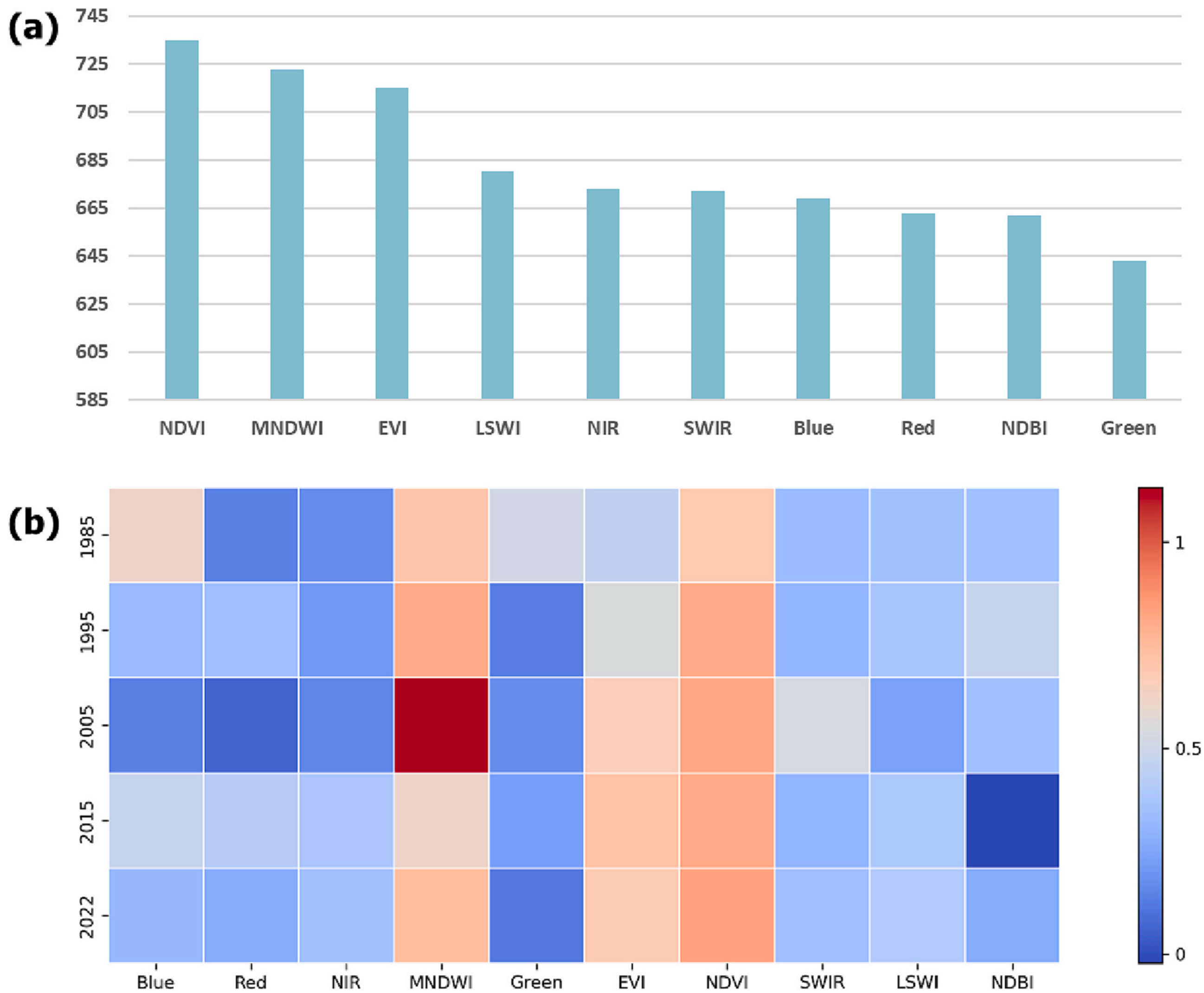

Fig. 4. (a) Variable importance ranking for RF classification, and (b) heatmap for multi-year variables efficiency.

for gains in area coverage of wetlands.

4. Discussion

4.1. Wetlands changes and its drivers in the Sylhet division

In the context of providing spatial-temporal baseline data for wetland-related investigations (e.g., carbon storage and wetland sustainability), this study integrates remote sensing, geo-information modelling, and machine learning approaches. The results from this study provide valuable information having important implications for decisions and policies regarding wetland conservation. The observed decline in wetlands reflects the loopholes in government policies to cause wetland losses along with highlighting the ill-managed wetland-rich regions. From Fig. 7, it is evident that around 45% of wetlands degradation took place between 1985 and 2022 whereas, the vegetation and dense vegetation classes showed an increase of ~9 and 15%, respectively. Hence, there has been a land-use shifting pattern in the region in the last few decades. While this study showed vegetation class as a significant contributing factor to wetland decline, a framework was needed to identify the affected regions. Therefore to aid sustainable conservation and restoration activities, this study further quantifies areas with the highest wetland degradation at the lowest sub-administration level (Upazila or sub-districts). Therefore, we evaluated the area percent change aggregated to each Upazila boundary (Fig. 8). The highest decline in wetlands area is observed in four Upazila including *Jamalganj, Derai, Sulla, and Ajmiriganj*, with a decrease between −70 to −82% during 1985–2022. It is worth mentioning that to the best of our knowledge, no other study has addressed this issue of wetlands degradation for these regions (division, district, and sub-district) so far. Hence, the findings from this study further benchmark the baseline for future wetland investigations in this region.

While no study at the scale of our investigation is available to compare our findings in this region, several other studies have reported similar LULC changing trends. A recent study by Kafy et al. (2022), for instance, suggests that Sylhet city has experienced high urbanization (an increase of 10.1 km^2 in built-up areas) in the last 25 years at the expense of vegetation, water, and barren land. On the contrary, at the sub-district or upper administration level, vegetation plays a significant role because agriculture is the primary occupation for ~90% of residents in adjoining rural areas (World Bank, 2016). This indicates how agriculture is responsible for most of the land-use shifting patterns when one moves from core cities to sub-district and upper administrative levels (Waleed and Sajjad, 2022). Hence, it is reasonable to say that the conversion of wetlands to agriculture-related economic activities could further deteriorate the overall situation of wetlands in the regions—resulting in the loss of diverse services. For this purpose, the findings from this study provide important references (i.e., the regions with larger transitions

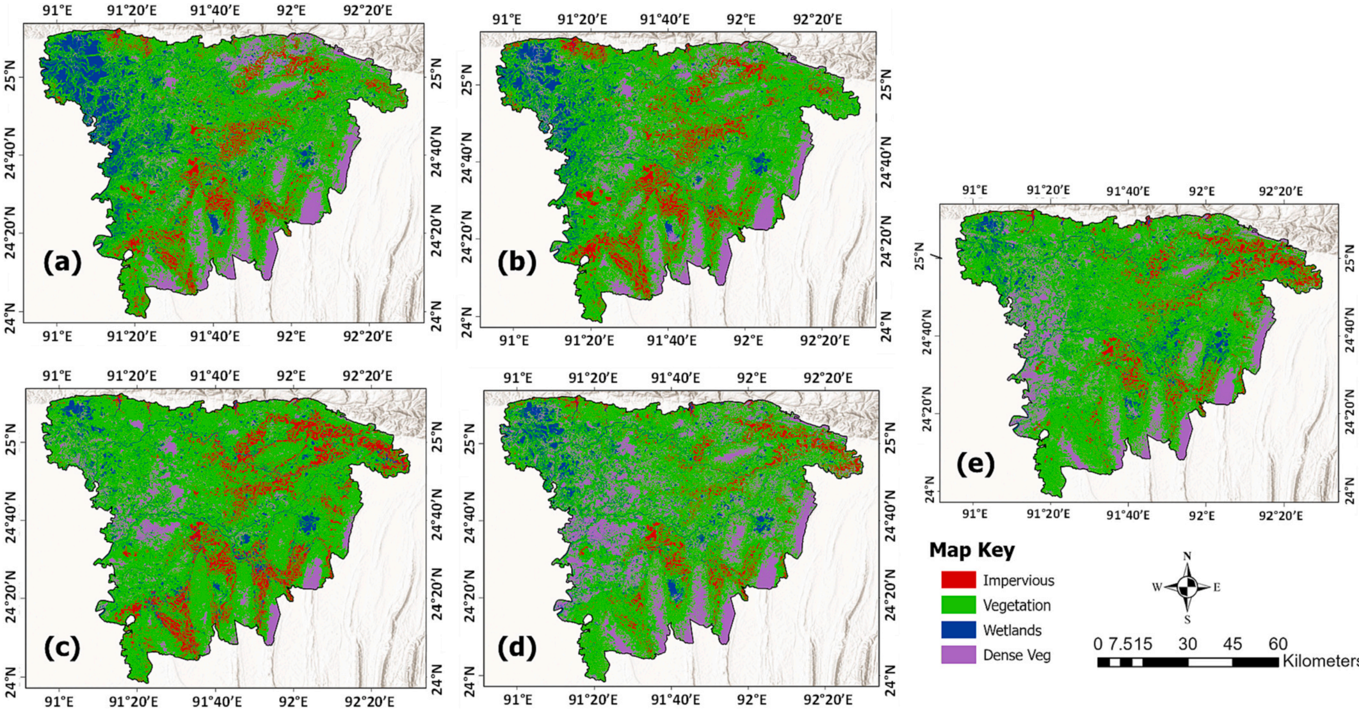

Fig. 5. Wetland land-use maps for Sylhet for (a) 1985–87, (b) 1995–97, (c) 2005–07, (d) 2015–17, and (e) 2020–2022.

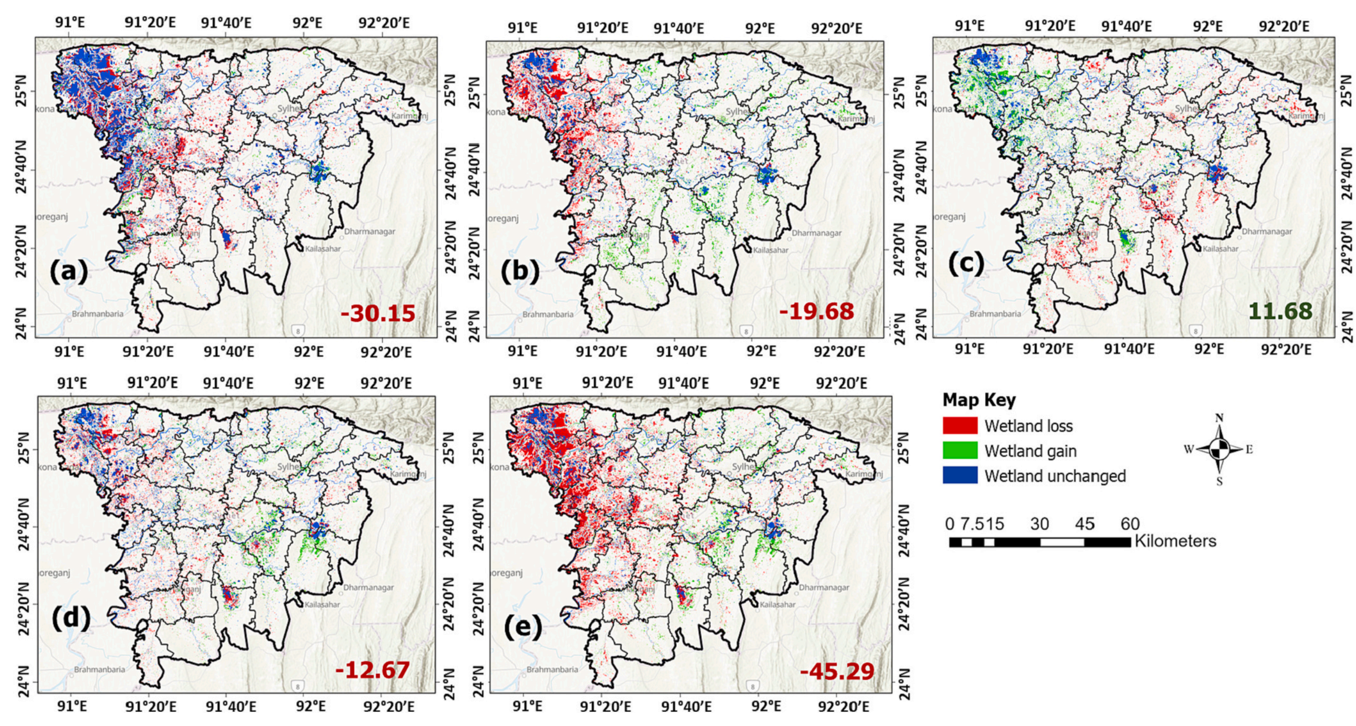

Fig. 6. Wetlands change detection analysis for (a) 1985–95, (b) 1995–2005, (c) 2005–15, (d) 2015–22, and (e) 1985–2022. Note that the dark and light black boundaries represent the Sylhet division and sub-districts of the Sylhet region respectively. Additionally, the coloured numbers in each map frame represent overall wetland class percent change (%), where red represents a decline and green shows improvement. (For interpretation of the references to color in this figure legend, the reader is referred to the web version of this article.)

from wetlands to agricultural land; Fig. 7).

While there are few previous studies (Hassan, 2017; Md. N. Islam et al., 2018; Salauddin and Islam, 2011) that addressed wetland area change-related issues at the local scale, almost all lack in addressing the wetland gain or loss trends in the region. Another important gap is the wetland transition analysis, which is equally important to analyze the conversion of wetlands into other land-use types and vice-versa. Among these aforementioned studies, only Salauddin and Islam (2011) highlighted the increase in vegetative (agricultural) land and the decrease in the wetland area. But at the same time, there is no systematic determination of the factors behind the decline of wetlands. In this context, while the wetland loss results from this study are in line with existing

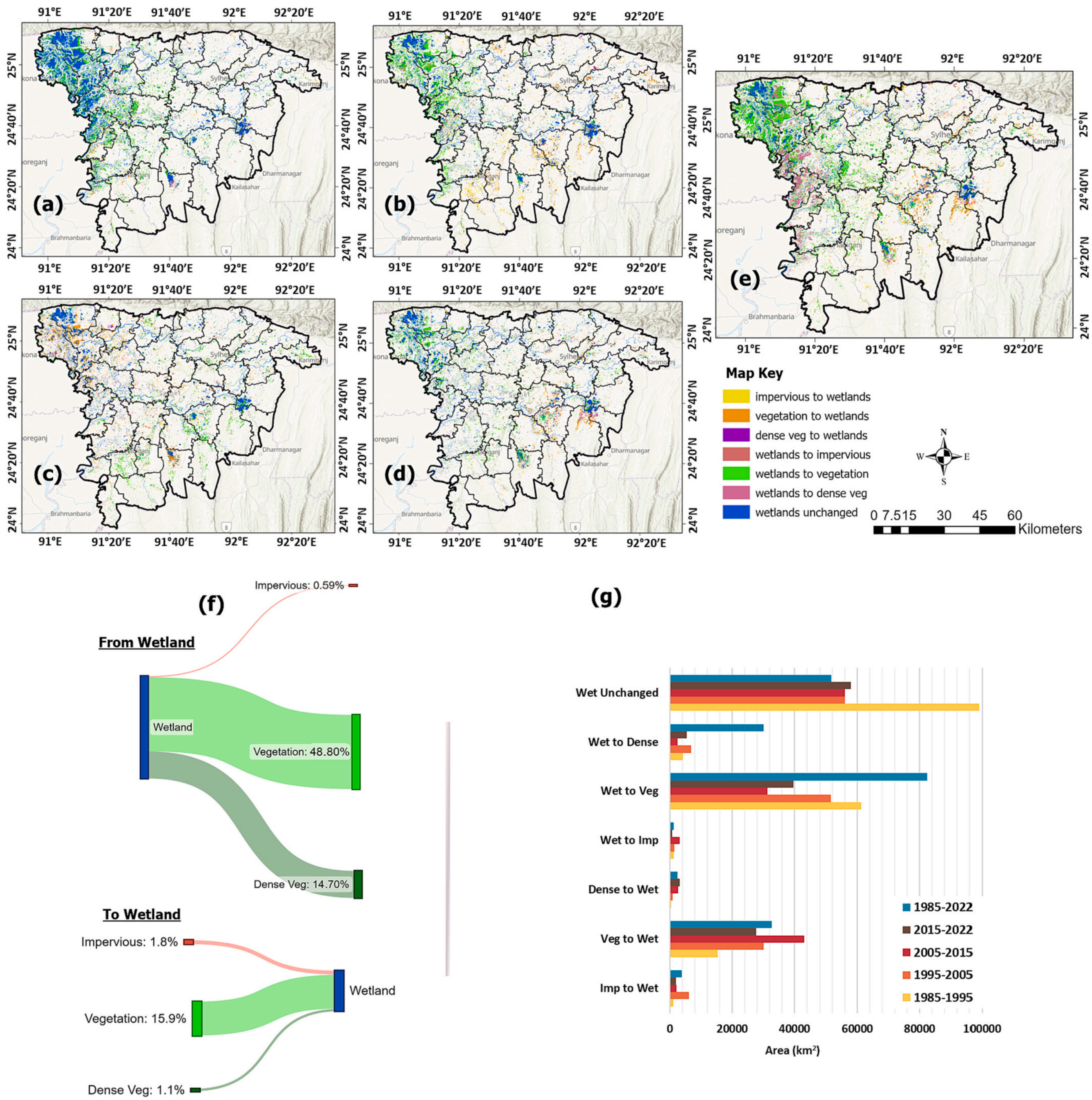

Fig. 7. Wetlands transition maps for (a) 1985–95, (b) 1995–2005, (c) 2005–15, (d) 2015–22, and (e) 1985–2022. Note that the dark and light black boundaries represent the division and districts of the Sylhet region. (f) shows Sankey diagrams of changes of wetland in percentage from and to different classes for the 1985–2022 period and (g) shows transition area changes for each decade and the overall 1985–2022 period.

literature, the identification of the driving factors responsible for this decline (Fig. 7) is particularly useful for effective measures.

4.2. Limitations and the way forward

While this study performed wetland mapping with good accuracy, some limitations are important to discuss. The first is the unavailability of wetlands inventory data, which could be used for training and validation purposes. In developed countries, such data are provided by government or private bodies mostly free of charge. If not, many datasets are collected through field campaigns using government-provided funding. Such data include detailed point or polygon geolocation samples for different wetland classes (swamps, marshes, bog, fen). For example, Mahdianpari et al. (2020a, 2020b) evaluated spatial-temporal patterns of different wetlands classes in Newfoundland (Canada) using 432 wetland polygon samples collected during field surveys from 2015 to 2017. They highlighted the issue of budget and time constraints for arranging different field surveys. Although such data are necessary for detailed and sub-classes-based classification of wetlands, it is difficult to map wetland classes with good accuracy in the absence of such inventories, especially for larger regions like the Sylhet division. Therefore, to counter this issue, this study considered wetlands as the main

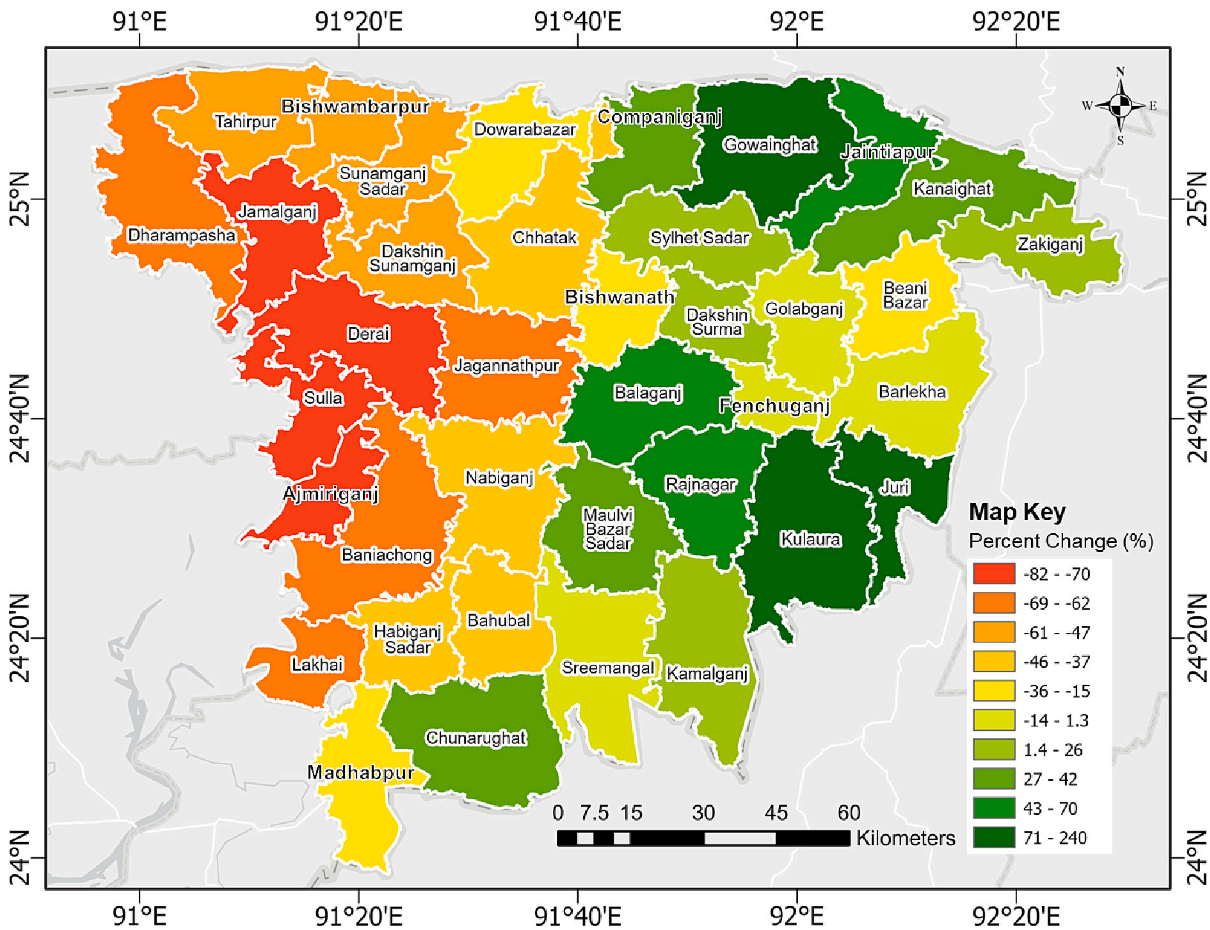

Fig. 8. Wetland area change (percent) during 1985 and 2022 aggregated to each Upazila boundary.

class containing merged subclasses, such as swamps, marshes, bog, fen, and open water. Once such ground truths become available, the produced maps of wetlands as a result of this study could be updated and refined for further comprehensiveness and accuracy.

Another issue associated with wetland classification is the cloud coverage issue. When using multispectral images (such as from Landsat mission satellites), cloud presence severely degrades data quality and results in abrupt pixel values, which could lead to classification bias (Waleed and Sajjad, 2022). While previous studies support the use of microwave satellite data such as Sentinel-1, which can penetrate through clouds (Singha et al., 2020), such techniques are computationally intensive. Furthermore, the data are only available for the previous six to eight years, which is not aligned with the scope of this study and hinders establishing long-term wetland analysis. Hence, the data catalogue of Landsat, reaching back as far as the 1980s, is utilized. Thus, to deal with the cloud cover issue, we choose images from three years between the pre-monsoon months (January, February, and March) with minimum cloud coverage (<10%) for each composite. Furthermore, to make a completely cloud-free composite, we removed every cloudy pixel using the quality assessment Landsat band as mentioned in the methodology section.

For variable importance analysis (Fig. 4), it was observed that some SIs showed comparatively higher importance than others. This phenomenon may be due to water sensitivity towards the near infrared region of electromagnetic spectrum. Due to this, water appears as a darker pixel, when captured by the near-infrared sensor of a satellite. These darker pixels can be easily separated using simple threshold techniques (Ji et al., 2009). However, due to the similarity of clouds and shadow reflectance with water reflectance, noise is created, and water pixels are not correctly extracted. Thus, SIs are developed using multiple bands to get better object delineation (Bijeesh and Narasimhamurthy, 2019). In our case, SIs also proved crucial as they aided in the improved classification of the wetlands.

From the viewpoint of methodology, we found that the RF classifier is the optimal choice, which is also preferred for its proven results in several other regions of the world (Guo et al., 2017; Mahdavi et al., 2018; Masoud Mahdianpari et al., 2020b). Hence, future studies can employ the RF technique to investigate wetlands. The primary reason for RF's improved accuracy is that it works on the principle of decision trees, in which each tree is divided into multiple features until a decision is finalized. In this process, features are randomly divided, and the model only considers small subset of features. This process ensures that variance can be averaged (Pelletier et al., 2016). Such ability of RF makes it robust despite of smaller sample size and provides good decision accuracy in most conditions.

Creating multi-temporal and highly accurate wetland maps is important to acquire knowledge about the past and current wetland-rich regions, which ultimately helps in proper monitoring and conservation-related initiatives by concerned departments (DeLancey et al., 2022). The wetlands change transition analysis from this study also provided spatial and quantitative insights regarding the conversion of different LULC classes. While such wetland classification techniques are already applied in many developed regions of the world, the development of further robust and cost-effective wetland mapping techniques is always encouraged (Mahdavi et al., 2018). With the development of new techniques, it is equally important to apply existing techniques to other areas of the world prone to wetland degradation. Doing this will ultimately provide wetland gain or loss-related insights for different periods providing support for corrective decisions in the context of wetland sustainability (Guo et al., 2017). Additionally, such change detection data would allow concerned agencies to further evaluate the transparency of government policies implemented time-to-time and will reflect their actions in the past regarding wetland conservation.

5. Conclusion

Wetlands are important ecosystems because of their multiple advantages to humans and the environment. Therefore, monitoring and sustaining wetlands should be the utmost priority of the concerned authorities. Wetlands in the Sylhet division are home to many rare and endangered species requiring the government's intention to take necessary initiatives to preserve them. This study concludes that satellite-based time series data and machine learning algorithms are particularly useful and cost-effective for the classification of wetlands in the context of their sustainability—particularly in developing areas of the world where monitoring costs are a major constraint. Classification of the study area has been done by different methods and the results are compared for all the methods. It is evident that RF is a highly accurate method for the classification of wetlands as compared with other approaches (i.e., SVM, CART, and MD). This study also highlights the variation in the area coverage of wetlands and all other classes including vegetation, impervious, and dense vegetation. Our findings conclude that wetlands have experienced instability over the past four decades with ~45% net loss. Most of this wetland loss is the consequence of the transition of wetlands to vegetation land (82,000 km^2 transition). The variations in other classes have also been analyzed and the statistical analysis shows that transitional changes to agricultural land are the most important factor in the loss of wetlands. The recent decline in wetlands further highlights that the government initiatives in the past were not adequate regarding wetlands conservation—particularly in the western regions of the study area. To restore wetlands in the region, the government and decision-makers should concentrate their efforts in those areas that experienced high wetland declines, as shown in this study. Finally, future research should focus on the loss of ecosystem services (i.e., water purification, erosion, flood control, and carbon storage) and patterns and trends assessment of loss and gain in carbon storage at several geographical scales. This study could potentially act as a stepping-stone towards such investigations.

Declaration of Competing Interest

None.

Data availability

All the data and software used in this research are freely available and the resources are mentioned within the paper. ArcGIS Pro. is used for post processing of the results and maps production, and could be obtained from the Environmental Systems Research Institute (www.esri.com).

Appendix A. Supplementary data

Supplementary data to this article can be found online at https://doi.org/10.1016/j.ecoinf.2023.102075.

References

Adam, E., Mutanga, O., Rugege, D., 2010. Multispectral and hyperspectral remote sensing for identification and mapping of wetland vegetation: a review. Wetl. Ecol. Manag. 18, 281–296. https://doi.org/10.1007/s11273-009-9169-z.

Amani, M., Brisco, B., Afshar, M., Mirmazloumi, S.M., Mahdavi, S., Mirzadeh, S.M.J., Huang, W., Granger, J., 2019a. A generalized supervised classification scheme to produce provincial wetland inventory maps: an application of Google Earth Engine for big geo data processing. Big Earth Data 3, 378–394. https://doi.org/10.1080/20964471.2019.1690404.

Amani, M., Mahdavi, S., Afshar, M., Brisco, B., Huang, W., Mirzadeh, S.M.J., White, L., Banks, S., Montgomery, J., Hopkinson, C., 2019b. Canadian wetland inventory using Google Earth Engine: the first map and preliminary results. Remote Sens. 11, 1–20. https://doi.org/10.3390/RS11070842.

Anand, V., Oinam, B., 2020. Future land use land cover prediction with special emphasis on urbanization and wetlands. Remote Sens. Lett. 11, 225–234. https://doi.org/10.1080/2150704X.2019.1704304.

Bhowmik, S., 2020. Ecological and economic importance of wetlands and their vulnerability: a review. Curr. State Futur. Impacts Clim. Chang. Biodivers. 95–112.

Bijeesh, T.V., Narasimhamurthy, K.N., 2019. A comparative study of spectral indices for surface water delineation using Landsat 8 images. In: 2019 International Conference on Data Science and Communication (IconDSC). Presented at the 2019 International Conference on Data Science and Communication (IconDSC), pp. 1–5. https://doi.org/10.1109/IconDSC.2019.8816929.

Chatterjee, K., Bandyopadhyay, A., Ghosh, A., Kar, S., 2015. Assessment of environmental factors causing wetland degradation, using Fuzzy analytic network process: a case study on Keoladeo National Park, India. Ecol. Model. 316, 1–13. https://doi.org/10.1016/j.ecolmodel.2015.07.029.

Chowdhury, C., Karim, M.R., Sayed, C.M.A.A., Uddin, C.M.N., Kamal, C.M.M., Suhrab, C.M.I.R., 2022. A study on the marine environment, conservation measures, and compliance of policy in Bangladesh perspective. J. Coast. Life Med. 10, 07–27.

Cohen, J., 1960. A coefficient of agreement for nominal scales. Educ. Psychol. Meas. 20, 37–46. https://doi.org/10.1177/001316446002000104.

Congalton, R.G., 1991. A review of assessing the accuracy of classifications of remotely sensed data. Remote Sens. Environ. 37, 35–46. https://doi.org/10.1016/0034-4257(91)90048-B.

Dar, Shahid Ahmad, Bhat, S.U., Rashid, I., Dar, Sajad Ahmad, 2020. Current status of wetlands in Srinagar City: threats, management strategies, and future perspectives. Front. Environ. Sci. 7 https://doi.org/10.3389/fenvs.2019.00199.

DeLancey, E.R., Czekajlo, A., Boychuk, L., Gregory, F., Amani, M., Brisco, B., Kariyeva, J., Hird, J.N., 2022. Creating a detailed wetland inventory with Sentinel-2 time-series data and Google Earth Engine in the Prairie Pothole Region of Canada. Remote Sens. 14, 3401. https://doi.org/10.3390/rs14143401.

Dronova, I., 2015. Object-based image analysis in wetland research: a review. Remote Sens. 7, 6380–6413. https://doi.org/10.3390/rs70506380.

Guo, M., Li, J., Sheng, C., Xu, J., Wu, L., 2017. A review of wetland remote sensing. Sensors 17, 777. https://doi.org/10.3390/s17040777.

Haque, M.M., Bremer, S., Aziz, S.B., van der Sluijs, J.P., 2017. A critical assessment of knowledge quality for climate adaptation in Sylhet Division, Bangladesh. Clim. Risk Manag. 16, 43–58. https://doi.org/10.1016/j.crm.2016.12.002.

Hassan, M.M., 2017. Monitoring land use/land cover change, urban growth dynamics and landscape pattern analysis in five fastest urbanized cities in Bangladesh. Remote Sens. Appl. Soc. Environ. 7, 69–83. https://doi.org/10.1016/j.rsase.2017.07.001.

Hislop, S., Jones, S., Soto-Berelov, M., Skidmore, A., Haywood, A., Nguyen, T., 2018. Using landsat spectral indices in time-series to assess wildfire disturbance and recovery. Remote Sens. 10, 460. https://doi.org/10.3390/rs10030460.

Hoque, M.J., 2022. Causes, Mechanisms and Outcomes of Environmental Degradation in Bangladesh: A STUDY in Sylhet.

Hu, Q., Yang, B., Xie, L., Rosa, S., Guo, Y., Wang, Z., Trigoni, N., Markham, A., 2021. Learning semantic segmentation of large-scale point clouds with random sampling. IEEE Trans. Pattern Anal. Mach. Intell. https://doi.org/10.1109/TPAMI.2021.3083288.

Iqbal, M., Nasren, S., Al Mamun, M.A., Hossain, M., 2015. Fish assemblage including threatened species in Hakaluki haor, Sylhet. Bangladesh J. Aqua Trop. 30, 233–246.

Islam, S.N., 2010. Threatened wetlands and ecologically sensitive ecosystems management in Bangladesh. Front. Earth Sci. China 4, 438–448. https://doi.org/10.1007/s11707-010-0127-0.

Islam, Md.N., Rakib, M.R., Sufian, Md.A., Raihan Sharif, A.H.M., 2018. Detection of climate change impacts on the Hakaluki Haor wetland in Bangladesh by use of remote sensing and GIS. In: Islam, Md.N., van Amstel, A. (Eds.), Bangladesh I: Climate Change Impacts, Mitigation and Adaptation in Developing Countries. Springer Climate. Springer International Publishing, Cham, pp. 195–214. https://doi.org/10.1007/978-3-319-26357-1_8.

Ji, L., Zhang, L., Wylie, B., 2009. Analysis of dynamic thresholds for the normalized difference water index. Photogramm. Eng. Remote. Sens. 75, 1307–1317. https://doi.org/10.14358/PERS.75.11.1307.

Kafy, A.-A., Saha, M., Faisal, A.-A., Rahaman, Z.A., Rahman, M.T., Liu, D., Fattah, Md.A., Al Rakib, A., AlDousari, A.E., Rahaman, S.N., Hasan, M.Z., Ahasan, M.A.K., 2022. Predicting the impacts of land use/land cover changes on seasonal urban thermal characteristics using machine learning algorithms. Build. Environ. 217, 109066 https://doi.org/10.1016/j.buildenv.2022.109066.

Kaplan, G., Yigit Avdan, Z., Avdan, U., 2019. Mapping and monitoring wetland dynamics using thermal, optical, and SAR remote sensing data. Wetlands Manag. Assess. Risk Sustain. Sol. 87 https://doi.org/10.5772/intechopen.80264.

Mahdavi, S., Salehi, B., Granger, J., Amani, M., Brisco, B., Huang, W., 2018. Remote sensing for wetland classification: a comprehensive review. GISci. Remote Sens. 55, 623–658. https://doi.org/10.1080/15481603.2017.1419602.

Mahdianpari, M., Granger, J.E., Mohammadimanesh, F., Salehi, B., Brisco, B., Homayouni, S., Gill, E., Huberty, B., Lang, M., 2020a. Meta-analysis of wetland classification using remote sensing: a systematic review of a 40-year trend in North America. Remote Sens. 12 https://doi.org/10.3390/rs12111882.

Mahdianpari, M., Jafarzadeh, H., Granger, J.E., Mohammadimanesh, F., Brisco, B., Salehi, B., Homayouni, S., Weng, Q., 2020b. A large-scale change monitoring of wetlands using time series Landsat imagery on Google Earth Engine: a case study in Newfoundland. GISci. Remote Sens. 57, 1102–1124. https://doi.org/10.1080/15481603.2020.1846948.

Mallick, J., Talukdar, S., Pal, S., Rahman, A., 2021. A novel classifier for improving wetland mapping by integrating image fusion techniques and ensemble machine learning classifiers. Ecol. Informat. 65, 101426.

Pelletier, C., Valero, S., Inglada, J., Champion, N., Dedieu, G., 2016. Assessing the robustness of Random Forests to map land cover with high resolution satellite image time series over large areas. Remote Sens. Environ. 187, 156–168. https://doi.org/10.1016/j.rse.2016.10.010.

Prasai, R., Schwertner, T.W., Mainali, K., Mathewson, H., Kafley, H., Thapa, S., Adhikari, D., Medley, P., Drake, J., 2021. Application of Google earth engine python API and NAIP imagery for land use and land cover classification: A case study in Florida, USA. Ecol. Informat. 66, 101474.

Rashid, H.E., 2019. Geography of Bangladesh. Routledge, New York. https://doi.org/10.4324/9780429048098.

Rwanga, S.S., Ndambuki, J.M., 2017. Accuracy assessment of land use/land cover classification using remote sensing and GIS. IJG 08, 611–622. https://doi.org/10.4236/ijg.2017.84033.

Salauddin, M., Islam, A., 2011. Identification of land cover changes of the haor area of Bangladesh using Modis Images. In: Presented at the Proceedings of the 3rd International Conference on Water & Flood Management (ICWFM-2011). Institute of Water and Flood Management, BUET Dhaka, Bangladesh.

Sang, X., Guo, Q., Wu, X., Fu, Y., Xie, T., He, C., Zang, J., 2019. Intensity and stationarity analysis of land use change based on CART algorithm. Sci. Rep. 9, 1–12. https://doi.org/10.1038/s41598-019-48586-3.

Sasaki, Y., 2007. The truth of the F-measure. Teach Tutor Mater. 1, 1–5.

Shafi, A., Chen, S., Waleed, M., Sajjad, M., 2023. Leveraging machine learning and remote sensing to monitor long-term spatial-temporal wetland changes: towards a national RAMSAR inventory in Pakistan. Appl. Geogr. 151, 102868 https://doi.org/10.1016/j.apgeog.2022.102868.

Singha, M., Dong, J., Sarmah, S., You, N., Zhou, Y., Zhang, G., Doughty, R., Xiao, X., 2020. Identifying floods and flood-affected paddy rice fields in Bangladesh based on Sentinel-1 imagery and Google Earth Engine. ISPRS J. Photogramm. Remote Sens. 166, 278–293. https://doi.org/10.1016/j.isprsjprs.2020.06.011.

Ståhl, N., Weimann, L., 2022. Identifying wetland areas in historical maps using deep convolutional neural networks. Ecol. Informat. 68, 101557.

Sufian, M., Kunda, M., Islam, M., Haque, A., Pandit, D., 2017. Socioeconomic conditions of fishermen of Dekar Haor in Sunamganj. J. Sylhet Agril. Univ 4, 101–109.

Talukdar, S., Singha, P., Mahato, S., Shahfahad, Pal, S., Liou, Y.-A., Rahman, A., 2020. Land-use land-cover classification by machine learning classifiers for satellite observations—a review. Remote Sens. 12, 1135. https://doi.org/10.3390/rs12071135.

Tamiminia, H., Salehi, B., Mahdianpari, M., Quackenbush, L., Adeli, S., Brisco, B., 2020. Google Earth Engine for geo-big data applications: a meta-analysis and systematic review. ISPRS J. Photogramm. Remote Sens. 164, 152–170. https://doi.org/10.1016/j.isprsjprs.2020.04.001.

Waleed, M., Sajjad, M., 2022. Leveraging cloud-based computing and spatial modeling approaches for land surface temperature disparities in response to land cover change: evidence from Pakistan. Remote Sens. Appl. Soc. Environ. 25, 100665 https://doi.org/10.1016/j.rsase.2021.100665.

Waleed, M., Mubeen, M., Ahmad, A., Habib-ur-Rahman, M., Amin, A., Farid, H.U., Hussain, S., Ali, M., Qaisrani, S.A., Nasim, W., Javeed, H.M.R., Masood, N., Aziz, T., Mansour, F., EL Sabagh, A., 2022. Evaluating the efficiency of coarser to finer resolution multispectral satellites in mapping paddy rice fields using GEE implementation. Sci. Rep. 12, 13210. https://doi.org/10.1038/s41598-022-17454-y.

Waleed, M., Sajjad, M., Acheampong, A.O., Alam, M.T., 2023. Towards Sustainable and Livable Cities: Leveraging Remote Sensing, Machine Learning, and Geo-Information Modelling to Explore and Predict Thermal Field Variance in Response to Urban Growth. Sustainability 15 (2), 1416.

World Bank, 2016. Bangladesh: Growing the Economy through Advances in Agriculture. https://www.worldbank.org/en/results/2016/10/07/bangladesh-growing-economy-through-advances-in-agriculture.

Xu, T., Weng, B., Yan, D., Wang, K., Li, X., Bi, W., Li, M., Cheng, X., Liu, Y., 2019. Wetlands of international importance: status, threats, and future protection. Int. J. Environ. Res. Public Health 16, 1818. https://doi.org/10.3390/ijerph16101818.